

Magnonics along the wall in Bimeron Chain Domain Walls

Carlos Saji,¹ Eduardo Saavedra,² Roberto E. Troncoso,³ Mario A. Castro,¹ Sebastian Allende,^{2,4} and Alvaro S. Nunez¹

¹*Departamento de Física, FCFM, Universidad de Chile, Santiago, Chile.*

²*Departamento de Física, Universidad de Santiago de Chile, 9170124, Santiago, Chile.*

³*School of Engineering and Sciences, Universidad Adolfo Ibañez, Santiago, Chile*

⁴*Centro de Nanociencia y Nanotecnología CEDENNA, Avda. Ecuador 3493, Santiago, Chile.*

(Dated: December 10, 2024)

We demonstrate that domain walls built from bimeron chains (bc-DW) in two-dimensional systems constitute a spontaneously assembled medium that holds magnonic excitations along its direction. We prove that such magnons are topological, leading to protected edge states. We also verify the stability of the domain walls and its edge modes' resilience against disorder. Analytical calculations and micromagnetic simulations support our findings. The robustness of these edge modes holds promise for potential applications in the design of nanoscale magnonic devices for information storage and transport.

Introduction.— Spin waves, whose quanta are magnons, have attracted significant attention in recent years [1–6]. These are collective spin excitations in magnetically ordered materials, such as ferromagnets, ferrimagnets, and antiferromagnets [7, 8]. Due to their low energy consumption and long coherence lengths, spin waves and magnons are considered promising candidates for next-generation information carriers.

In a parallel development, topological band theory became a prominent area of research in condensed matter physics [9–13]. In the past decade, research on topological matter has gained substantial momentum. Topological matter exhibits non-trivial structures characterized by gapped behavior in the bulk and robust conducting states on their surfaces or edges. These edge or surface states hold significant promise for practical applications. Beyond electronic states, topological behavior has also been observed in other types of excitations. For example, photons [14], phonons [15], polaritons [16], and plasmons [17], among others, have been shown to host topological properties. From this perspective, topological magnonic systems and the nascent field of topological magnonics are precipitating a new range of effects, with potential applications in energy-efficient information technology [18–27].

Bimerons are topological spin textures stabilized by in-plane anisotropy in non-centrosymmetric ferromagnetic materials, exhibiting several properties with skyrmions [28–32]. In particular, they can form lattice-like structures and have recently been observed in open or closed chain formations [33, 34]. Bc-DWs have been highlighted for their distinctive dynamical behaviors, such as serving as a track for bimeron motion and their ability to mitigate the skyrmion Hall effect [35]. Additionally, domain-wall bimerons have been experimentally observed in various studies [36–38]. Recent research has also explored the interaction between spin waves and bimerons [39]. However, the topological phenomena associated with magnons in the vicinity of a bc-DW remain largely unexplored.

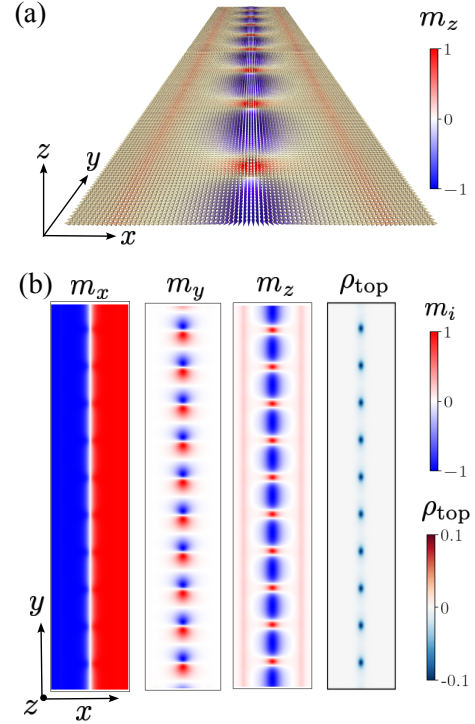


FIG. 1. Visualization of the bimeron chain domain wall. (a) Magnetization texture in the nanostripe, containing 10 bimerons distributed along the DW, and obtained through micromagnetic simulations in Mumax³. (b) Cartesian components of the magnetization and the topological density charge $\rho_{top} = \mathbf{m} \cdot (\partial_x \mathbf{m} \times \partial_y \mathbf{m})$ [nm^{-2}], where each bimeron has a topological charge $Q = -1$.

In this Letter we demonstrate, by performing micromagnetic simulations and analytical calculations of the magnonic states, that domain walls built based on bimeron chains in two-dimensional systems constitute a spontaneously assembled medium that, acting as a tunable magnonic metamaterial, holds topological edge modes. Although bulk modes function as magnonic waveguides, the robustness of these edge modes

holds promise for potential applications in the design of nanoscale devices for information storage and transport. In addition, we observe that bc-DWs and their topological edge modes remain stable against substantial magnetic disorder, introduced into the system in the form of Voronoi grains, highlighting their potential use in the design of spintronic devices. Our work bridges the gap in understanding topological phenomena associated with spin-wave modes of bc-DWs, providing valuable insights into the potential of these systems for hosting topologically protected magnonic modes.

Theoretical model.— We consider a chiral thin ferromagnetic material with in-plane magnetic anisotropy along the x -axis, with a rectangular geometry of dimensions L_x and L_y , as in Fig. 1. The magnetic energy density reads, $\mathcal{E} = \mathcal{E}_{\text{ex}} + \mathcal{E}_{\text{DMI}} + \mathcal{E}_K + \mathcal{E}_Z + \mathcal{E}_{\text{DDI}}$, where $\mathcal{E}_{\text{ex}} = A(\nabla \mathbf{m})^2$ represents the Heisenberg exchange, $\mathcal{E}_{\text{DMI}} = D(m_z(\nabla \cdot \mathbf{m}) - (\mathbf{m} \cdot \nabla)m_z)$ the interfacial Dzyaloshinskii–Moriya (DMI), $\mathcal{E}_K = K_u(1 - m_x^2)$ the in-plane easy-axis anisotropy along the x -direction, and $\mathcal{E}_Z = -B_y m_y$ the Zeeman coupling B_y a static global in-plane field. The dipolar field energy, $\mathcal{E}_{\text{DDI}} = -\mu_0 M_s \mathbf{H}_d \cdot \mathbf{m}/2$, is approximated as an effective anisotropy and a confining harmonic well for the domain wall. To pin the domain wall and prevent rigid displacements of the chain, we introduce an easy-axis surface anisotropy K_S along the x -direction at the boundaries $x = \pm L_x/2$. Let us introduce the polar representation (oriented to the x -axis), $\mathbf{m} = (\cos \Theta, \sin \Theta \sin \Phi, \sin \Theta \cos \Phi)$, and we consider the following ansatz for the bc-DW,

$$\Theta(x, y) = 2 \arctan \left[e^{-x/w + X(y)} \right], \quad \Phi(x, y) = \eta(y), \quad (1)$$

which corresponds to a set of domain walls (parametrized by the continuous y variable) with core position $wX(y)$ and chiral angle $\eta(y)$. The thickness of the DW is determined by $w = \sqrt{A/(2K_{\text{eff}})}$ [40], where the effective anisotropy $K_{\text{eff}} = K_u + 2\mu_0 M_s^2$ takes into account a significant contribution from the dipolar field.

Next, we determine the domain wall profile using $X(y, t)$ and $\eta(y, t)$ as collective variables, and by substituting the ansatz Eq. (1) into the magnetic energy density, we arrive at the effective energy of the bc-DW,

$$E[X, \eta] = \int [wA((\partial_y X)^2 + (\partial_y \eta)^2) + D \cos(\eta) + wB_y \sin(\eta) + U(X)] dy, \quad (2)$$

where $U(X)$ represents a pinning potential considering the shape anisotropy and the dipolar field on the bc-DW. Now, considering small deviations from the equilibrium position $X = 0$, we can model $U(X)$ as a one-dimensional harmonic potential $U(X) = k_{el} X^2$. To describe the effective dynamics, we determine the Lagrangian of the collective variables, $\mathcal{L}[X, \eta] = \mathcal{K}[X, \eta] - \gamma_0 E[X, \eta]$, with the kinetic energy, $\mathcal{K}[X, \eta] = \int G_{X\eta} X \partial_t \eta dy$, written in

terms of the gyrotropic tensor element between X and η ,

$$G_{X\eta} = \int \sin \Theta (\partial_X \Theta \partial_\eta \Phi - \partial_\eta \Theta \partial_X \Phi) d^2 x = w \int \sin \Theta \partial_x \Theta dx = 2w, \quad (3)$$

Thus, we obtain the Lagrangian for the collective dynamical conjugate variables,

$$\mathcal{L}[X, \eta] = \int [2wX \partial_t \eta - \gamma_0 wA((\partial_y X)^2 + (\partial_y \eta)^2) - \gamma_0 D \cos \eta - \gamma_0 wB_y \sin \eta - \gamma_0 k_{el} X^2] dy. \quad (4)$$

The Euler-Lagrange equation for X leads to $w \partial_t \eta = -\gamma_0 wA \partial_y^2 X + \gamma_0 k_{el} X$, which we solve using the Green function $\mathcal{G} = (k_{el} - wA \partial_y^2)^{-1}$ as $X = \gamma_0^{-1} w \mathcal{G} \partial_t \eta$. Under the assumption that the stiffness k_{el} is strong enough such that $wA \mathcal{G}_y^2 \ll k_{el}$, where $\mathcal{G}_y = 2\pi/\lambda$ and λ represent the period of the bc-DW; thus the Green's function becomes sufficiently local in space, and we can make the approximation $X = w/(\gamma_0 k_{el}) \partial_t \eta$. Substituting it into $\mathcal{L}[X, \eta]$, the new effective Lagrangian density is given by $\mathcal{L}_{\text{eff}}[\eta] = m_{\text{eff}}(\partial_t \eta)^2 - (\partial_y \eta)^2 - 2d \cos \eta - 2b \sin \eta$, with the effective mass $m_{\text{eff}} = w/(\gamma_0^2 k_{el} A)$, $d = D/(2wA)$, and $b = B_y/(2A)$. Therefore, the equilibrium configuration

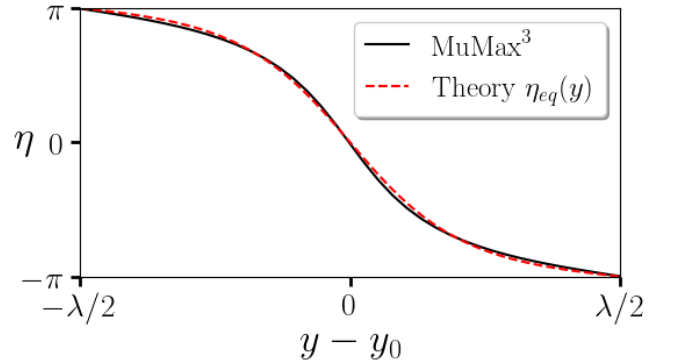


FIG. 2. Chiral angle η of a bc-DW along the DW symmetry axis $x = 0$ of Fig. 1. In the solid line is depicted the value of η according to the micromagnetic simulations in Mumax³, whereas in the dashed red line is plotted the theoretical prediction given at Eq. (6), with $\kappa = 0.99$ and $b = 0$. Analytical results are well consistent with the micromagnetic simulations.

satisfies the so-called sine-Gordon differential equation,

$$\frac{d^2 \eta_{eq}}{dy^2} = -\epsilon \sin(\eta_{eq} - \delta_b), \quad (5)$$

with $\epsilon = \sqrt{d^2 + b^2}$ and $\delta_b = \arctan(b/d)$. The solution of the differential equation in Eq. (5) can be expressed in terms of the Jacobi amplitude function, am [41, 42],

$$\eta_{eq}(y) = -2 \operatorname{am} \left(\sqrt{\frac{\epsilon}{\kappa}} (y - y_0), \kappa \right) + \delta_b, \quad (6)$$

where κ stands for the elliptic modulus. The solution at Eq. (6) defines a periodic magnetization profile $m_z(0, y) = \cos(\eta_{eq}(y))$ and $m_y(0, y) = \sin(\eta_{eq}(y))$, with the period given by $\lambda = 2K(\kappa)\sqrt{\kappa/\epsilon}$, where $K(\kappa) = \int_0^{\pi/2} (1 - \kappa^2 \sin^2 \theta)^{-1/2} d\theta$ denotes the complete elliptic integral of the first kind. More detailed information between the relation of λ and κ are found at the Supplementary Material. On the other hand, the constant y_0 is determined by the Neumann boundary conditions [43],

$$\frac{\partial \mathbf{m}}{\partial \mathbf{n}} = \frac{D}{2A} (\hat{\mathbf{z}} \times \mathbf{n}) \times \mathbf{m}, \quad (7)$$

where \mathbf{n} denotes the exterior normal vector to the boundary in the XY plane. Applying Eq. (7) with $\mathbf{n} = -\hat{\mathbf{y}}$ at $y = 0$, we obtain $\eta'(0) = D/(2A)$, hence $\sqrt{\epsilon/\kappa} \text{am}'(-\sqrt{\epsilon/\kappa} y_0, \kappa) = D/(2A)$, which can be solved numerically. We compare this result with the one obtained using Mumax³ for the chiral angle, see Fig. 2.

Spin wave spectrum.— We now focus in the study of small perturbations around the equilibrium solution η_{eq} . Expanding the Lagrangian $\mathcal{L}_{\text{eff}}[\eta]$ up to second order in $\delta\eta = \eta - \eta_{eq}$, we find the dynamics of linear excitations, which are determined by the eigenvalue problem,

$$\mathcal{H}\Psi = (-\partial_y^2 + V_{\text{eff}}(y)) \Psi = m_{\text{eff}}\omega^2 \Psi, \quad (8)$$

where $\Psi(\omega)$ is the Fourier transform of $\delta\eta(t)$. The effective potential $V_{\text{eff}}(y)$ is defined by,

$$V_{\text{eff}}(y) = -\epsilon \cos \left[2 \text{am} \left(\sqrt{\frac{\epsilon}{\kappa}} (y - y_0), \kappa \right) \right]. \quad (9)$$

We observe that it is a periodic potential with a period of λ . Furthermore, if $B_y = 0$, then we have that $V_{\text{eff}}(y) = -\epsilon \cos(\eta_{eq}(y)) = -\epsilon m_z(x = 0, y)$ attains its minimum and maximum values precisely at $m_z = 1$ and $m_z = -1$, respectively. This allows us to interpret the effective dynamics as analogous to those of a particle moving in a one-dimensional crystal with potential wells localized at the core of the bimerons of the chain.

Let us focus on the spectrum of the Hamiltonian \mathcal{H} . We first note that there is a zero energy mode $\Psi_0(y)$, which is described by $\Psi_0(y) = \eta'_{eq}(y)$. This mode is the Goldstone mode associated with the translational symmetry along the y -axis. Separately, stabilizing the equilibrium state defined by η_{eq} requires that all eigenvalues in Eq. (8) be non-negative, $\epsilon_n = m_{\text{eff}}\omega_n^2 \geq 0$. In fact, following the supersymmetric quantum mechanics approach (SUSY-QM) [44, 45], the Hamiltonian (8) can be written as $\mathcal{H} = A^\dagger A$, where the operator A is defined by $A = -\partial_y + W(y)$ with the superpotential $W(y) = \eta''_{eq}(y)/\eta'_{eq}(y)$. This implies that the \mathcal{H} spectrum is nonnegative. See the Supplementary Material for more details. This technique has previously been used in magnonics [46, 47]. Moreover, using the SUSY-QM correspondence, we can calculate an approximate solution

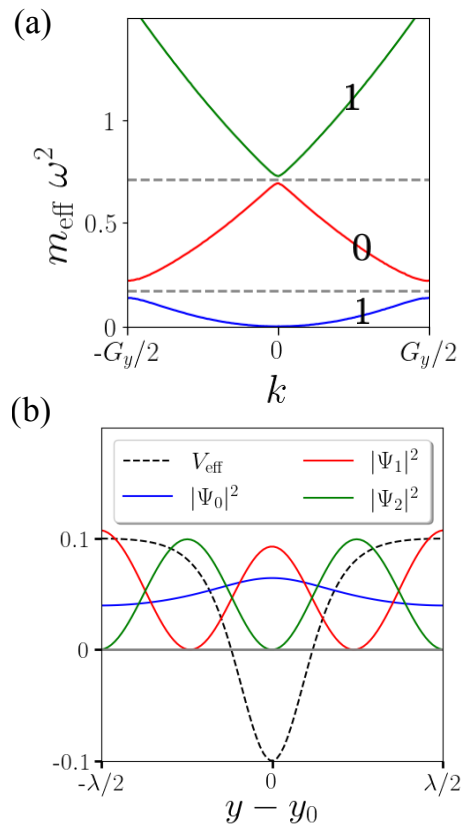


FIG. 3. (a) Spectrum of the Hamiltonian $\mathcal{H}(k)$ obtained by solving the eigenvalue problem in Eq. (12). The effective potential V_{eff} is defined in Eq. (9) with parameters $\kappa = 0.99$ and $\epsilon = 0.1$. The respective Zak phase $\gamma_n \in \{0, 1\}$ is marked on each band. The horizontal dashed lines represent topological band gaps. We note that the spectrum is indeed positive. (b) Normal modes $\Psi_n(y)$ calculated by solving Eq. (12) with periodic boundary conditions ($k = 0$). In color, solid lines show the amplitude of the mode $\Psi_{n=0,1,2}$. The dashed line represents the effective potential at Eq. (9) with parameters $\kappa = 0.99$ and $\epsilon = 0.1$.

for the Bloch eigenfunctions of $\mathcal{H}(k)$ in the asymptotic case $\kappa \approx 1$, we obtain the following result,

$$\Psi_{n,k}(y) \approx (W(y) - i(k + nG_y)) e^{i(k+nG_y)(y-y_0)} \quad (10)$$

$$m_{\text{eff}}\omega_{n,k}^2 \approx (k + nG_y)^2 + \epsilon. \quad (11)$$

In the general case, we determine the band structure through the exact diagonalization procedure as follows: we begin by writing the Fourier expansion of a Bloch wave $\Psi_k(y) = \frac{1}{\sqrt{N}} \sum_{n=-N}^N e^{i(k+nG_y)(y-y_0)} \psi_n$, where $N \rightarrow \infty$. Substituting in Eq. (8), the secular equation reads,

$$\sum_m \left[(k + nG_y)^2 \delta_{nm} + V_{n-m} \right] \psi_m = m_{\text{eff}}\omega^2 \psi_n, \quad (12)$$

where $V_n = \frac{1}{\lambda} \int_{-\lambda/2}^{\lambda/2} e^{inG_y(y-y_0)} V_{\text{eff}}(y) dy$ are the Fourier coefficients of V_{eff} , which we calculate in the Supplemen-

tary Material. The above system is solved numerically, from which we illustrate the lower-energy normal modes $\Psi_{n=0,1,2}(y)$ with periodic boundary conditions ($k = 0$), and their associated band spectrum in Fig. 3.

The topology of the bands is characterized by the Zak phase [48], defined by the integral of the Berry connection [49] over the Brillouin zone (BZ),

$$\gamma_n = \frac{i}{\pi} \oint_{BZ} \left\langle \Psi_n(k) \left| \frac{\partial}{\partial k} \Psi_n(k) \right. \right\rangle dk \pmod{2}$$

The matrix Hamiltonian $\mathcal{H}(k)$ defined by Eq. (12) satisfies the symmetry $\mathcal{I}\mathcal{H}(k)\mathcal{I}^{-1} = \mathcal{H}(-k)$, with $\mathcal{I} = \mathcal{P}_y\mathcal{K}$, where \mathcal{P}_y is the parity operator $\mathcal{P}_y\psi_n = \psi_{-n}$, and \mathcal{K} is the element wise complex conjugation operation. As a result of the symmetry protection, the Zak phase is quantized [50], taking values of $\gamma_n = 0$ or $\gamma_n = 1$ depending on whether the n -th band is trivial or topological, respectively.

The Zak phase for the lower energy modes is indicated in Fig. 3. Here, $\gamma_0 = 1$ is provided for the lower energy band and $\gamma_1 = 0$ for the upper band, and $\gamma_2 = 1$ for the next band. Consequently, we conclude that there are two topological band gaps in the proposed model. In contrast, under open boundary conditions, the edge-bulk correspondence implies that the non-trivial topology results in the presence of edge modes with energies within the topological gap. In the next section, we compare these theoretical predictions with micromagnetic numerical simulations, confirming the appearance of edge modes at the ends of the bc-DW. Finally, it is worth noting that in the case $B_y = 0$ and $D/A \ll w$, we have that $\epsilon \approx 0$, thereby the effective potential can be approximated, at first order in ϵ , as $V_{\text{eff}}(y) = -\epsilon \cos(\frac{D}{2A}y + \eta_0)$ (see Supplementary Material), which gives rise to a non-trivial topological structure with topological edge states, whenever the potential shift $\eta_0 \pmod{\pi}$ is nonzero [51].

Micromagnetic simulations.— The simulations were performed using the GPU-accelerated micromagnetic software package Mumax³ [52], which solve Landau-Lifschitz-Gilbert (LLG) equation,

$$\partial_t \mathbf{m} = -\gamma \mathbf{m} \times \mathbf{H}_{\text{eff}} + \alpha \mathbf{m} \times \partial_t \mathbf{m} \quad (13)$$

where γ is the electron gyromagnetic ratio, α is the Gilbert damping constant, and the effective field is given by $\mu_0 \mathbf{H}_{\text{eff}} = -\partial_{\mathbf{m}} \mathcal{E} / M_s$. The dimensions of the geometry are $L_x = 80$ nm and $L_y = 400$ nm. The cell size is $1 \times 1 \times 1$ nm³. The magnetic parameters used in the simulations are as follows: exchange stiffness constant $A_{\text{ex}} = 15$ pJ/m, saturation magnetization $M_{\text{sat}} = 580$ kA/m, $D = 3$ mJ/m², easy-axis anisotropy along the x -direction from $K_u = 500$ kJ/m³, boundary anisotropy $K_S = 1$ mJ/m², and the damping constant $\alpha = 0.005$. We initialize the magnetization of a bc-DW containing N bimerons using the ansatz $\Theta(x, y) = \pi/2 (1 - \tanh(x/w))$ (domain wall far from the

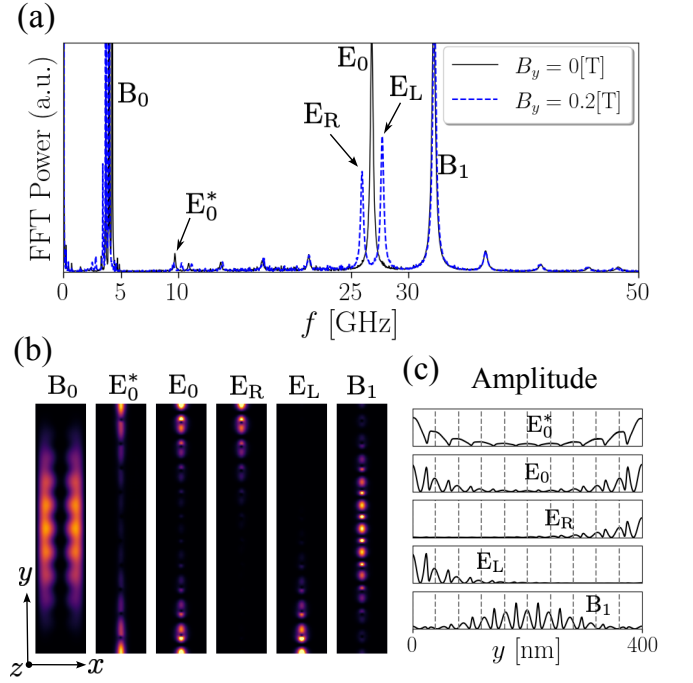


FIG. 4. Spin waves modes of a bc-DW, with $N = 10$ bimerons (see Fig. 1). (a) Ferromagnetic spectrum for external magnetic fields $B_y = 0$ and $B_y = 0.2$ T. For the case $B_y = 0$, the observed modes are E_0, E_0^*, B_0, B_1 , whereas for $B_y = 0.2$ T, the modes are E_L, E_R, B_0, B_1 . (b) The local mode amplitude in color code. (c) The mode amplitude along the symmetry axis $x = 0$ of the bc-DW.

center) and $\Phi(x, y) = -2\pi Ny/L_y$. The system is then relaxed to the equilibrium state. The energy of a bc-DW as a function of its number of bimerons is illustrated in the Supplementary Material.

The spin wave spectrum of a bc-DW is found by analyzing the power spectrum of the dynamical response of magnetization $\delta \mathbf{m}(\mathbf{r}, t) = \mathbf{m}(\mathbf{r}, t) - \mathbf{m}(\mathbf{r}, t = 0)$, under a uniform sinc magnetic field $\mathbf{B}(t) = B_0 \sin(2\pi f_{\text{max}}(t - t_0)) / (2\pi f_{\text{max}}(t - t_0)) \mathbf{y}$ of strength $B_0 = 1$ mT and the cutoff frequency of $f_{\text{max}} = 50$ GHz, and $t_0 = 1$ ns. Then we determine the spatial FFT distribution as the Fourier image of each magnetic moment excitation $\delta \mathbf{m}_\omega(x, y) = \text{DFTt}(\delta \mathbf{m}(x, y, t))$, where DFTt is the discrete-time Fourier transform. Fig. 4 shows the resonance frequencies and their corresponding spatial FFT amplitude distributions for the cases $B_y = 0$ and $B_y = 0.2$ T. The observed modes are categorized into two groups. (i) Bulk modes, displaying an extended amplitude on the geometry, here in both cases, $B_y = 0$ and $B_y = 0.2$ T, we see the modes B_0, B_1 ; (ii) Edge localized modes, denoted by E_0^*, E_0 , for the case $B_y = 0$, and E_L, E_R if $B_y = 0.2$ T. We observe that the energy of the edge mode E_0^* lies within the observed band gap between 5 GHz and 10 GHz, while the energies of the edge modes E_0, E_L, E_R lie within the band gap between 25 GHz and 30 GHz. These results support the predictions of our the-

oretical model, confirming the topological nature of the described modes. We can also note the appearance of energy splitting associated with the edge states E_L and E_R when B_y does not vanish. We attribute this effect to the breaking of inversion symmetry, analogous to the energy splitting of edge modes in the Rice-Mele model [53].

Resilience of edge modes.— In this section, we explore the robustness of edge modes against the disorder effect. We introduce magnetic inhomogeneities into the system in the form of Voronoi grains of average size 20 nm, such that each grain had a uniformly distributed anisotropy strength of $K_u(\mathbf{r}) = K_u + \chi(\mathbf{r})\Delta K_u$, where $-1 < \chi(\mathbf{r}) < 1$ is a random number defined over each grain in the region. In our simulations, we set $K_u = 500$ kJ/m³ and $\Delta K_u = 0.1 K_u$. The spectrum of the disordered system is

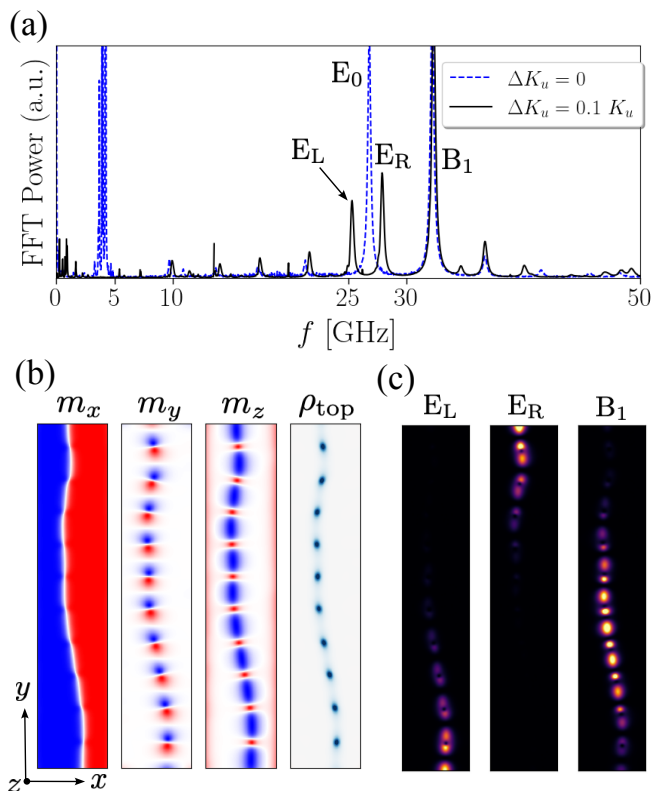


FIG. 5. Magnonics Modes in a bc-DW with disorder anisotropy. (a) Ferromagnetic spectrum for the homogeneous case $\Delta K_u = 0$ (it is the same as the case $B_y = 0$ in the figure 4), and with anisotropy disorder $\Delta K_u = 0.1 K_u$. In the disordered case, we report the existence of the two edge modes E_L, E_R . (b) Components x, y, z of the magnetization and the topological density charge for the disordered case. (c) The local mode amplitude in color code.

shown in Fig. 5. Notably, the edge states remain stable even when the domain wall significantly deviates from the symmetry axis due to the random inhomogeneities.

Conclusions.— We demonstrate that the domain walls of bimeron chains support topologically protected

magnonic edge modes, making them candidates for magnon-based information transfer. A bc-DW serves as a remarkable example of a magnonic topological waveguide, which exhibits unique edge modes. As we show, these edge modes stand out for their remarkable resilience against a variety of external disturbances, making them particularly appealing for technological applications. This robustness is not an accident; it arises from the intricate design of the bc-DW, which creates a distinctive structure that supports these protected states.

The potential applications of these edge modes are vast, especially in the realm of nanotechnology. One of the most exciting possibilities lies in their use for the development of advanced nanodevices aimed at highly efficient data storage solutions built based on the localized magnon states with exceptional stability, which can effectively manage and transport information with increased reliability and efficiency. Thus, domain walls of bimeron chains represent an important advance in the search for innovative technologies in information storage and transmission.

Acknowledgments.— A.S.N. and R.E.T. acknowledges funding from Fondecyt Regular 1230515 and 1230747, respectively. C.S. thanks the financial support provided by the ANID National Doctoral Scholarship N^o21210450. M.A.C. acknowledges Proyecto ANID Fondecyt de Postdoctorado 3240112. E.S. acknowledges support from Dicyt-USACH 042331SD.

-
- [1] B. Flebus, S. M. Rezende, D. Grundler, and A. Barman, “Recent advances in magnonics,” *Journal of Applied Physics* **133** (2023), 10.1063/5.0153424.
 - [2] A. Roldán-Molina, Alvaro S. Nunez, and R. A. Duine, “Magnonic black holes,” *Phys. Rev. Lett.* **118**, 061301 (2017).
 - [3] R. J. Doornenbal, A. Roldán-Molina, A. S. Nunez, and R. A. Duine, “Spin-wave amplification and lasing driven by inhomogeneous spin-transfer torques,” *Phys. Rev. Lett.* **122**, 037203 (2019).
 - [4] R. Hidalgo-Sacoto, R. I. Gonzalez, E. E. Vogel, S. Allende, José D. Mella, C. Cardenas, Roberto E. Troncoso, and F. Munoz, “Magnon valley hall effect in cri₃-based van der waals heterostructures,” *Physical Review B* **101** (2020), 10.1103/physrevb.101.205425.
 - [5] Philipp Pirro, Vitaliy I. Vasyuchka, Alexander A. Serga, and Burkard Hillebrands, “Advances in coherent magnonics,” *Nature Reviews Materials* **6**, 1114–1135 (2021).
 - [6] J. S. Harms, H. Y. Yuan, and Rembert A. Duine, “Antimagnonics,” *AIP Advances* **14** (2024), 10.1063/5.0151652.
 - [7] Charles Kittel, *Quantum theory of solids*, 2nd ed. (John Wiley & Sons, Nashville, TN, 1987).
 - [8] Charles Kittel, *Introduction to solid state physics*, 8th ed. (John Wiley & Sons, Nashville, TN, 2004).
 - [9] F. Duncan M. Haldane, “Nobel lecture: Topological

- quantum matter,” *Rev. Mod. Phys.* **89**, 040502 (2017).
- [10] John Michael Kosterlitz, “Nobel lecture: Topological defects and phase transitions,” *Rev. Mod. Phys.* **89**, 040501 (2017).
- [11] Roderich Moessner and Joel E. Moore, *Topological Phases of Matter* (Cambridge University Press, 2021).
- [12] M. Z. Hasan and C. L. Kane, “Colloquium: Topological insulators,” *Reviews of Modern Physics* **82**, 3045–3067 (2010).
- [13] Xiao-Liang Qi and Shou-Cheng Zhang, “Topological insulators and superconductors,” *Reviews of Modern Physics* **83**, 1057–1110 (2011).
- [14] Hannah Price, Yidong Chong, Alexander Khanikaev, Henning Schomerus, Lukas J Maczewsky, Mark Kremer, Matthias Heinrich, Alexander Szameit, Oded Zilberberg, Yihao Yang, Baile Zhang, Andrea Alù, Ronny Thomale, Iacopo Carusotto, Philippe St-Jean, Alberto Amo, Avik Dutt, Luqi Yuan, Shanhui Fan, Xuefan Yin, Chao Peng, Tomoki Ozawa, and Andrea Blanco-Redondo, “Roadmap on topological photonics,” *Journal of Physics: Photonics* **4**, 032501 (2022).
- [15] Yuanfeng Xu, M. G. Vergniory, Da-Shuai Ma, Juan L. Mañes, Zhi-Da Song, B. Andrei Bernevig, Nicolas Regnault, and Luis Elcoro, “Catalog of topological phonon materials,” *Science* **384** (2024), 10.1126/science.adf8458.
- [16] Torsten Karzig, Charles-Edouard Bardyn, Netanel H. Lindner, and Gil Refael, “Topological polaritons,” *Phys. Rev. X* **5**, 031001 (2015).
- [17] Yanan Dai, Zhikang Zhou, Atreyie Ghosh, Roger S. K. Mong, Atsushi Kubo, Chen-Bin Huang, and Hrvoje Petek, “Plasmonic topological quasiparticle on the nanometre and femtosecond scales,” *Nature* **588**, 616–619 (2020).
- [18] Ryuichi Shindou, Ryo Matsumoto, Shuichi Murakami, and Jun-ichiro Ohe, “Topological chiral magnonic edge mode in a magnonic crystal,” *Physical Review B* **87** (2013), 10.1103/physrevb.87.174427.
- [19] A Roldán-Molina, A S Nunez, and J Fernández-Rossier, “Topological spin waves in the atomic-scale magnetic skyrmion crystal,” *New Journal of Physics* **18**, 045015 (2016).
- [20] Esteban Aguilera, R. Jaeschke-Ubiergo, N. Vidal-Silva, Luis E. F. Foa Torres, and A. S. Nunez, “Topological magnonics in the two-dimensional van der waals magnet CrI_3 ,” *Phys. Rev. B* **102**, 024409 (2020).
- [21] A T Costa, D L R Santos, N M R Peres, and J Fernández-Rossier, “Topological magnons in CrI_3 monolayers: an itinerant fermion description,” *2D Materials* **7**, 045031 (2020).
- [22] R. Jaeschke-Ubiergo, E. Suárez Morell, and A. S. Nunez, “Theory of magnetism in the van der waals magnet CrI_3 ,” *Phys. Rev. B* **103**, 174410 (2021).
- [23] X. S. Wang and X. R. Wang, “Topological magnonics,” *Journal of Applied Physics* **129** (2021), 10.1063/5.0041781.
- [24] Paul A. McClarty, “Topological magnons: A review,” *Annual Review of Condensed Matter Physics* **13**, 171–190 (2022).
- [25] M. dos Santos Dias, N. Biniskos, F. J. dos Santos, K. Schmalzl, J. Persson, F. Bourdarot, N. Marzari, S. Blügel, T. Brückel, and S. Lounis, “Topological magnons driven by the dzyaloshinskii-moriya interaction in the centrosymmetric ferromagnet Mn_5Ge_3 ,” *Nature Communications* **14** (2023), 10.1038/s41467-023-43042-3.
- [26] Carlos Saji, Roberto E. Troncoso, Vagson L. Carvalho-Santos, Dora Altbir, and Alvaro S. Nunez, “Hopfion-driven magnonic hall effect and magnonic focusing,” *Phys. Rev. Lett.* **131**, 166702 (2023).
- [27] Alonso Tapia, Carlos Saji, Alejandro Roldán-Molina, and Alvaro S. Nunez, “Stability enhancement by zero-point spin fluctuations: A quantum perspective on Bloch point topological singularities,” *Advanced Functional Materials* **34** (2024), 10.1002/adfm.202312721.
- [28] Y. A. Kharkov, O. P. Sushkov, and M. Mostovoy, “Bound states of skyrmions and merons near the Lifshitz point,” *Phys. Rev. Lett.* **119**, 207201 (2017).
- [29] Börge Göbel, Alexander Mook, Jürgen Henk, Ingrid Mertig, and Oleg A. Tretiakov, “Magnetic bimerons as skyrmion analogues in in-plane magnets,” *Phys. Rev. B* **99**, 060407 (2019).
- [30] N. Gao, S. G. Je, M. Y. Im, J. W. Choi, M. Yang, Q. Li, T. Y. Wang, S. Lee, H. S. Han, K. S. Lee, W. Chao, C. Hwang, J. Li, and Z. Q. Qiu, “Creation and annihilation of topological meron pairs in in-plane magnetized films,” *Nature Communications* **10** (2019), 10.1038/s41467-019-13642-z.
- [31] Börge Göbel, Ingrid Mertig, and Oleg A. Tretiakov, “Beyond skyrmions: Review and perspectives of alternative magnetic quasiparticles,” *Physics Reports* **895**, 1–28 (2021).
- [32] M. A. Castro, D. Altbir, D. Galvez-Poblete, R. M. Corona, S. Oyarzún, A. R. Pereira, S. Allende, and V. L. Carvalho-Santos, “Skyrmion-bimeron dynamic conversion in magnetic nanotracks,” *Phys. Rev. B* **108**, 094436 (2023).
- [33] Natsuki Mukai and Andrey O. Leonov, ““polymerization” of bimerons in quasi-two-dimensional chiral magnets with easy-plane anisotropy,” *Nanomaterials* **14**, 504 (2024).
- [34] Xichao Zhang, Jing Xia, Laichuan Shen, Motohiko Ezawa, Oleg A. Tretiakov, Guoping Zhao, Xiaoxi Liu, and Yan Zhou, “Static and dynamic properties of bimerons in a frustrated ferromagnetic monolayer,” *Physical Review B* **101** (2020), 10.1103/physrevb.101.144435.
- [35] Jiwen Chen, Laichuan Shen, Hongyu An, Xichao Zhang, Hua Zhang, Haifeng Du, Xiaoguang Li, and Yan Zhou, “Magnetic bimeron traveling on the domain wall,” (2024).
- [36] Tomoki Nagase, Yeong-Gi So, Hayata Yasui, Takafumi Ishida, Hiroyuki K. Yoshida, Yukio Tanaka, Koh Saitoh, Nobuyuki Ikarashi, Yuki Kawaguchi, Makoto Kuwahara, and Masahiro Nagao, “Observation of domain wall bimerons in chiral magnets,” *Nature Communications* **12** (2021), 10.1038/s41467-021-23845-y.
- [37] Zhuolin Li, Jian Su, Shi-Zeng Lin, Dan Liu, Yang Gao, Shouguo Wang, Hongxiang Wei, Tongyun Zhao, Ying Zhang, Jianwang Cai, and Baogen Shen, “Field-free topological behavior in the magnetic domain wall of ferromagnetic gdfco ,” *Nature Communications* **12** (2021), 10.1038/s41467-021-25926-4.
- [38] Yuki Amari, Calum Ross, and Muneto Nitta, “Domain-wall skyrmion chain and domain-wall bimerons in chiral magnets,” *Phys. Rev. B* **109**, 104426 (2024).
- [39] Xue Liang, Jin Lan, Guoping Zhao, Mateusz Zelent, Maciej Krawczyk, and Yan Zhou, “Bidirectional magnon-driven bimeron motion in ferromagnets,” *Physical Review B* **108** (2023), 10.1103/physrevb.108.184407.

- [40] Se Kwon Kim and Oleg Tchernyshyov, “Mechanics of a ferromagnetic domain wall,” *Journal of Physics: Condensed Matter* **35**, 134002 (2023).
- [41] N I Akhiezer, *Elements of the theory of elliptic functions*, Translations of mathematical monographs (American Mathematical Society, Providence, RI, 1990).
- [42] E. T. Whittaker and G. N. Watson, *A Course of Modern Analysis* (Cambridge University Press, 1996).
- [43] S. Rohart and A. Thiaville, “Skyrmion confinement in ultrathin film nanostructures in the presence of dzyaloshinskii-moriya interaction,” *Physical Review B* **88** (2013), 10.1103/physrevb.88.184422.
- [44] C V Sukumar, “Supersymmetric quantum mechanics of one-dimensional systems,” *Journal of Physics A: Mathematical and General* **18**, 2917–2936 (1985).
- [45] Fred Cooper, Avinash Khare, and Uday Sukhatme, “Supersymmetry and quantum mechanics,” *Physics Reports* **251**, 267–385 (1995).
- [46] A.L. González, P. Landeros, and Álvaro S. Núñez, “Spin wave spectrum of magnetic nanotubes,” *Journal of Magnetism and Magnetic Materials* **322**, 530–535 (2010).
- [47] Seungho Lee and Se Kwon Kim, “Generation of magnon orbital angular momentum by a skyrmion-textured domain wall in a ferromagnetic nanotube,” *Frontiers in Physics* **10** (2022), 10.3389/fphy.2022.858614.
- [48] J. Zak, “Berry’s phase for energy bands in solids,” *Phys. Rev. Lett.* **62**, 2747–2750 (1989).
- [49] M. V. Berry, “Quantal phase factors accompanying adiabatic changes,” *Proceedings of the Royal Society of London. A. Mathematical and Physical Sciences* **392**, 45–57 (1984).
- [50] Wladimir A. Benalcazar, B. Andrei Bernevig, and Taylor L. Hughes, “Electric multipole moments, topological multipole moment pumping, and chiral hinge states in crystalline insulators,” *Physical Review B* **96** (2017), 10.1103/physrevb.96.245115.
- [51] Yi Zheng and Shi-Jie Yang, “Topological bands in one-dimensional periodic potentials,” *Physica B: Condensed Matter* **454**, 93–97 (2014).
- [52] Arne Vansteenkiste, Jonathan Leliaert, Mykola Dvornik, Mathias Helsen, Felipe Garcia-Sanchez, and Bartel Van Waeyenberge, “The design and verification of mumax3,” *AIP Advances* **4** (2014), 10.1063/1.4899186.
- [53] M. J. Rice and E. J. Mele, “Elementary excitations of a linearly conjugated diatomic polymer,” *Phys. Rev. Lett.* **49**, 1455–1459 (1982).